ELSEVIER

European Journal of Radiology 45 (2003) 214–222

EJR
EUROPEAN JOURNAL OF RADIOLOGY

www.elsevier.com/locate/ejrad

Diffusion-weighted magnetic resonance imaging for monitoring diffusion changes in rectal carcinoma during combined, preoperative chemoradiation: preliminary results of a prospective study

Patrick A. Hein [a,b,*], Christian Kremser [c], Werner Judmaier [c], Jürgen Griebel [d], Karl-Peter Pfeiffer [e], Alfons Kreczy [f], Eugen B. Hug [b], Peter Lukas [a], Alexander F. DeVries [a]

[a] *Department of Radiotherapy and Radiooncology, University of Innsbruck, Innsbruck, Austria*
[b] *Department of Radiation Oncology, Dartmouth-Hitchcock Medical Center, 1 Medical Center Drive, Lebanon, NH 03756, USA*
[c] *Department of Magnetic Resonance, University of Innsbruck, Innsbruck, Austria*
[d] *Federal Office for Radiation Protection (BfS), Institute of Radiation Hygiene, Neuherberg, Germany*
[e] *Department of Biostatistics, University of Innsbruck, Innsbruck, Austria*
[f] *Department of Pathology, University of Innsbruck, Innsbruck, Austria*

Received 13 February 2002; received in revised form 2 August 2002; accepted 5 August 2002

Abstract

Purpose: To evaluate the clinical value of diffusion-weighted magnetic resonance imaging (DW-MRI) to monitor response of primary carcinoma of the rectum to preoperative chemoradiation by measuring tumor apparent diffusion coefficient (ADC). *Materials and methods:* Diffusion data of nine patients undergoing preoperative combined chemoradiation for clinical staged T3, N_{0-2}, M_0 carcinoma of the rectum were analyzed. Diffusion-weighted echo-planar MR images were obtained prior to and at specified intervals during chemoradiation and ADCs calculated from acquired tumor images. *Results:* Comparison of mean ADC and cumulative radiation dose showed a significant decrease of mean ADC at the 2nd ($P = 0.028$), 3rd ($P = 0.012$), and 4th ($P = 0.008$) weeks of treatment. Cytotoxic edema and fibrosis were considered as reasons for ADC decrease. *Conclusion:* This study demonstrated tumor ADC changes via detection of therapy-induced alterations in tumor water mobility. Our results indicate that diffusion-weighted imaging may be a valuable clinical tool to diagnose the early stage of radiation-induced fibrosis.

Keywords: Diffusion-weighted magnetic resonance imaging; Chemoradiation; Carcinoma of the rectum; Apparent diffusion coefficient

1. Introduction

MR scanning in cancer therapy is commonly used to determine the involvement of macroscopic structures for tumor diagnosis and staging. Functional MRI studies are increasingly applied to add information about changes in tumor pathophysiology, e.g. tumor microcirculation before and during radiotherapy [1,2]. Monitoring microscopic tumor behavior during a course of therapy, on the other hand, is mainly dependent on invasive methods and hence not part of clinical routine. A non-invasive method to supply this desirable information through the measurement of water proton mobility in tumor tissue is diffusion-weighted magnetic resonance imaging (DW-MRI).

By applying a pair of strong magnetic field gradient pulses within the imaging sequence [3] imaging is sensitized to random spin displacements of diffusing free water molecules [4]. The apparent diffusion coefficient (ADC) can be calculated from DWI measure-

* Corresponding author. Present address: Department of Radiation Oncology, Dartmouth-Hitchcock Medical Center, 1 Medical Center Drive, Lebanon, NH 03756, USA. Tel.: +1-603-650-6614; fax: +1-603-650-6616

E-mail address: patrick.a.hein@hitchcock.org (P.A. Hein).

0720-048X/02/$ - see front matter
PII: S0720-048X(02)00231-0

ments. ADCs depend on the impediment to free diffusion of water molecules in a single voxel [5] due to restricting barriers such as membranes, macromolecules and fibers inside different tissue compartments. Therefore, diffusion-weighted MRI has been suggested as a tool to distinguish different tissue compartments [6] and to detect changes in cellular tissue structure, which could be used to monitor effects of radiation in tumor tissue.

Tissue ADC is thought to be composed by mainly independent contributions of the extracellular (ECV, extracellular volume) and intracellular (ICV, intracellular volume) tissue compartments [7]. Due to the higher content of relatively impermeable impeding barriers like cell and nuclear membranes, organelles, cytoskeleton and matrix fibers, lower ADCs were reported in the intracellular compartment [8]. Thus, ADC changes are thought to reflect changes of the ECV/ICV ratio, whereby increased ICV leads ultimately to a lower ADC.

DWI has evolved as a highly sensitive imaging modality in the early detection of cerebral infarction. It is based on the observation of decreased ADCs caused by the reduced ECV/ICV ratio due to cytotoxic intracellular edema [9–11]. A reduction of intracellular proton movement due to energy loss during ischemia was considered as alternate explanation. Increased capillary permeability led to an increased ECV/ICV ratio with increased ADCs as observed in interstitial edema [12]. The loss of membrane integrity in necrotic tissue [13,14] changes the ratio in a similar manner. Apoptotic cell death as therapy effect has been reported to increase the ADC in an experimental study [15]. High amounts of fibers are capable to reduce apparent diffusion established by studies in muscle and white matter of the brain [16,17]. To our knowledge, data about the response of solid malignant tumors to fractionated radiotherapy are still missing. At present, studies demonstrating alterations of tumor ADCs [15,18,19] after therapy are based on experimental tumor models and obtained solely by pre- and post-therapeutic DWI measurements.

The fact that the above-described mechanisms influencing tissue ADC could determine tumor ADC during therapy encouraged us to employ this technique in a standardized, clinical, radiooncological setting. We hypothesized that if tumor diffusion coefficients obtained during therapy could be related to well-known, radiobiological, dose-dependent radiation effects [20,21], it might provide non-invasively obtained information about immediate therapy-induced changes in microscopic tissue structure. The aim of this study was to investigate the clinical value of measuring intratumoral ADCs by DWI during the entire course of combined preoperative chemoradiation in patients with primary rectal carcinoma.

2. Materials and methods

2.1. Patient population

Between January 1999 and October 2000, nine patients with carcinoma of the rectum participated in this prospective study. Included in this study were all 19- to 75-year-old patients at our institution diagnosed with primary, histopathologically proven adenocarcinoma of the rectum who underwent preoperative chemoradiation. Only patients with cT3 and histological grade G2 were eligible (see Table 1). The selected staging/grading combination led to the largest achievable homogeneous patient population . Patients with other T-stages or grades, metastatic spread, tumor invasion of the sphincter or current or prior second malignancies were excluded. Also excluded were patients who had previously undergone chemotherapy, abdominal surgery, or irradiation. The tumor spread (T-stage) was assessed by intrarectal ultrasonography (US) and/or computed tomography. Infiltration of perirectal fat was present in all patients. The clinical and histopathologic classification and stage grouping were in accordance with TNM classification [22].

Each patient received combined hyperfractionated chemoradiation preoperatively with total radiation doses ranging between 38.3 and 44 Gy; doses of 1.1 Gy per fraction were administered twice daily. 5-Fluorouracil (350 mg/m^2) was continuously administered via an implanted Port-A-Cath Deltec CADD-1 system (SIMS Deltec, Inc., St. Paul, MN) on each treatment day. Radiation fields in a 3-field technique (PA and two lateral fields [23]) included the rectal canal and adjacent lymph nodes. Each combined chemoradiation regimen started on Monday, and was interrupted on weekends. Following 4 weeks of treatment, the patients had a recovery interval of 2 weeks and underwent surgery thereafter.

For each tumor, therapy outcome was censored as "response", if treatment resulted in down-staging from clinical stage T3 to pathological stage pT0–2, i.e. if the postsurgical pathological observation revealed no invasion into the perirectal fat (pT0–2). "Non-response" implied persistence of perirectal invasion (pT3). Detailed patient data are summarized in Table 1.

The study was approved by the Institutional Review Board (University of Innsbruck). Written informed consent was obtained from all patients.

2.2. Diffusion-weighted magnetic resonance imaging

DWI was performed using a 1.5 T whole-body scanner (Magnetom Vision Plus; Siemens, Erlangen, Germany) equipped with a phased-array body coil.

For this study, a single shot spin-echo type of echo-planar sequence that provided diffusion weighting in the

Table 1
Patients and treatment characteristics

Patient No./age (years)	Preoperative stage[a]	Total dose at preoperative chemoradiation[b] (Gy)	Surgical treatment	Postoperative stage[a]
1/40	$CT_3N_1M_0$	39.4	Abdominoperineal resection	$ypT_2N_1M_0$
2/67	$CT_3N_0M_0$	39.4	Abdominoperineal resection	$ypT_2N_2M_0$
3/65	$CT_3N_2M_0$	39.9	Abdominoperineal resection	$ypT_2N_2M_0$
4/47	$CT_3N_0M_0$	38.3	Low anterior resection	$ypT_0N_0M_0$
5/59	$CT_3N_0M_0$	43.6	Abdominoperineal resection	$ypT_3N_1M_0$
6/55	$CT_3N_0M_0$	44	Abdominoperineal resection	$ypT_3N_0M_0$
7/55	$CT_3N_1M_0$	39.4	Abdominoperineal resection	$ypT_3N_0M_0$
8/38	$CT_3N_2M_0$	43.8	Abdominoperineal resection	$ypT_3N_0M_0$
9/57	$CT_3N_0M_0$	39.6	Low anterior resection	$ypT_3N_0M_0$

[a] Staging according to TNM classification [14].
[b] Doses of 1.1 Gy were administered twice a day.

direction of slice selection was used. The corresponding b-values to the diffusion sensitizing gradients were $b =$ 30, 300, 1100 s/mm^2. By using sequential k-space sampling, the effective echo time amounted to 123 ms and the bandwidth to 1250 Hz/pixel. Images were acquired with a matrix of 128×128 interpolated to 256×256 during image calculation. The measurement contained 20 consecutive slices at slice thickness of 5 mm, a slice gap of 1 mm and a field of view of 300 mm to cover the entire tumor extension. The acquisition time for each individual b-value and a stack of 20 slices was 4 s.

To calculate ADC maps from the three differently diffusion-weighted measurements, a linear regression model was used based on the logarithm of signal intensities as follows:

$$S(b) = S(0)\exp(-b\ \mathrm{ADC}),$$

where $S(b)$ represents the signal intensity with diffusion gradient, $S(0)$ the signal intensity without diffusion gradient and b the gradient factor (in s/mm^2) of the used pulse sequence, as a measure of strength of the diffusion gradient [6]. ADC maps were calculated and transferred to a remote PC workstation.

2.3. Imaging protocol and analysis

The initial MR imaging was performed prior to the start of radiation therapy and was repeated at constant intervals once weekly during the course of treatment. Prior to mapping, patients received an intravenous injection of 20 mg Buscopan® (Boehringer Ingelheim KG, Ingelheim, Germany) to minimize peristaltic movement.

The weekly imaging protocol included diffusion-weighted sequences and multiplanar T1-weighted sequences with and without Gadolinium-DTPA (Magnevist®, Schering, Berlin, Germany) enhancement using a standard turbo spin-echo sequence (repetition time/echo time, 800 ms/12 ms; turbo factor, 3; acquisition matrix, 256; field of view, 300–350 mm; slice thickness, 5 mm; slice gap, 1.5 mm; number of slices, 15). The total time for each study, including the acquisition of T1-weighted images was approximately 20 min. The ADC map of the largest tumor extension was included in further analyses. Regions of interest (ROI) were drawn manually in the ADC maps, using the corresponding, enhanced T1-weighted images in transverse orientation to identify the tumor regions by one of the authors (P.A.H.) who was not involved in direct patient care and unaware of therapeutic outcome. EPI sequences as used for DWI are prone to inherent geometric distortions. Therefore, ROIs were not directly copied from the T1-weighted image to the ADC map.

2.4. Statistical analysis

Statistical analysis was performed using SPSS 10.0 (SPSS, Cary, NC). Due to some deviations from a normal distribution, nonparametric procedures were applied. Paired comparisons were performed by using the Wilcoxon test. Since this study aimed at identifying trends and substantial changes, no P-value adjustments for multiple testing were performed. The correlation between succeeding values was evaluated by using the Spearman's rank correlation coefficient at a significance level of $P < 0.05$.

3. Results

Diffusion data from nine patients were obtained at five weekly measurement points. Representative T1-weighted and diffusion-weighted images are shown in Fig. 1; representative ADC maps during treatment are shown in Fig. 2. Data from two (4%) measurement points ($n = 45$) were excluded due to technical measurement errors. No treatment had to be interrupted for therapeutic reasons or incidence of side-effects $>$ Grade 2 according to the Radiation Therapy Oncology Group and the European Organization for Research and Treatment of Cancer [24]. Image quality of the acquired

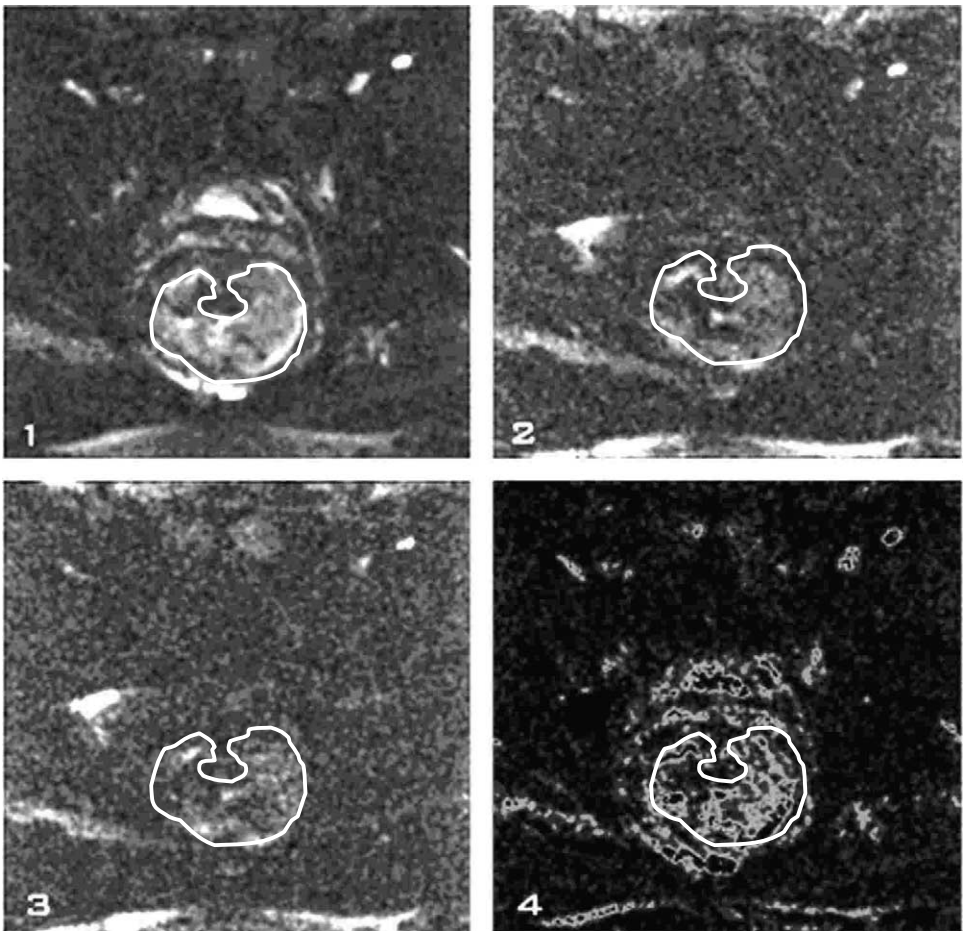

Fig. 1. (1–3) Axial diffusion-weighted MR images with b factors 30, 300, and 1100 s/mm^2, respectively (effective echo time, 123 ms; field of view, 300 mm; matrix, 128/256) of the measurement plane obtained in patient No. 6. (4) Resulting axial ADC map calculated from different diffusion-weighted images. White outlines indicate tumor region. Bright areas indicate high ADC values.

ADC maps was sufficient to identify the tumor region in all patients.

Mean ADC slightly increased from $0.755 \pm 0.155 \times 10^{-3}$ mm^2/s (95% CI: (0.636–0.874) $\times 10^{-3}$ mm^2/s) to $0.758 \pm 0.135 \times 10^{-3}$ mm^2/s (95% CI: (0.645–0.871) $\times 10^{-3}$ mm^2/s) in the 1st week. During further treatment mean ADC decreased continuously to $0.643 \pm 0.155 \times 10^{-3}$ mm^2/s (95% CI: (0.554–0.732) $\times 10^{-3}$ mm^2/s) in the 2nd week, $0.583 \pm 0.099 \times 10^{-3}$ mm^2/s (95% CI: (0.500–0.665) $\times 10^{-3}$ mm^2/s) in the 3rd week and $0.554 \pm 0.084 \times 10^{-3}$ mm^2/s (95% CI: (0.490–0.618) $\times 10^{-3}$ mm^2/s) in the 4th week (Figs. 3 and 4). The weekly observed ADCs of the nine patients are shown in Table 2.

At measurement points in the 1st and 3rd week in each case, one data point was missing due to technical errors. Thus, 100% of patients refer to total of nine patients ($n = 9$) at the pre-therapeutical measurement, the 2nd week, 4th week and to total of eight patients ($n = 8$) at the 1st and 3rd weeks. During the 1st week, six (75%) patients had a decrease in ADC compared with pretreatment values; eight (89%) patients had lower values in the 2nd week, eight (100%) patients had lower values in the 3rd week, and all nine patients (100%) demonstrated lower values in the 4th week (Fig. 3).

Comparison of mean ADC showed a significant decrease during the 2nd ($-0.112 \pm 0.125 \times 10^{-3}$ mm^2/s; 95% CI: (-0.209 to 0.016) $\times 10^{-3}$ mm^2/s; $P = 0.028$), 3rd ($-0.140 \pm 0.072 \times 10^{-3}$ mm^2/s; 95% CI: (-0.200 to 0.080) $\times 10^{-3}$ mm^2/s; $P = 0.012$) and 4th ($-0.201 \pm 0.088 \times 10^{-3}$ mm^2/s; 95% CI: (-0.268 to 0.134) $\times 10^{-3}$ mm^2/s; $P = 0.008$) weeks of treatment compared with pre-treatment levels. Changes measured in the 1st week ($-0.009 \pm 0.114 \times 10^{-3}$ mm^2/s; 95% CI: (-0.104 to 0.087) $\times 10^{-3}$ mm^2/s; $P = 0.624$) did not reach significance (Table 3).

Subsequent tumor resection permitted correlation of our findings with postsurgical, histopathologic staging. Down-staging of the T-stage occurred in four of nine patients (44%; Table 1). ADCs were decreased in 4/4 patients with pathologically observed down-staging of T-stage. ADCs were also decreased in 5/5 patients without down-staging of T-stage. Two patients (Nos. 3 and 9) demonstrated increased ADCs in the 1st week.

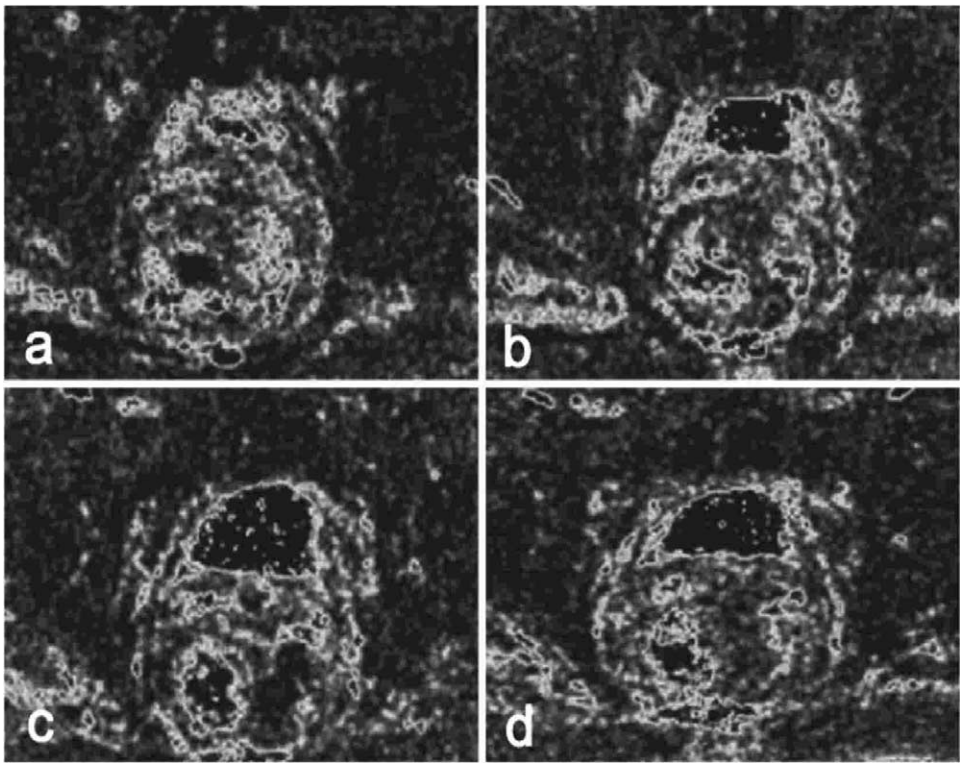

Fig. 2. (a–d) Representative axial ADC maps of the pelvis (patient No. 6) obtained during the course of treatment (weeks 1–4). Bright areas indicate high ADC values.

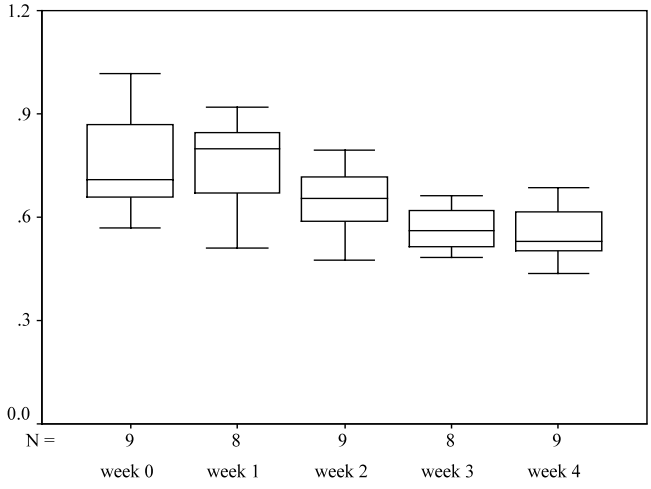

Fig. 3. Box-and-whiskers plots (median, the whiskers indicate the 5 or 95% quantal) of ADCs during chemoradiation.

This increase was accompanied by down-staging in T-stage of one patient, and no change in the other patient (Tables 1 and 2).

The correlation of weekly measured mean ADC and improvement in T-stage was not significant. Further statistical evaluation regarding therapy outcome was not performed due to the small patient number.

The pathohistological observation of hematoxylin–eosin stained slices showed an increased amount of fibrous tissue and a dense lymphocytic infiltrate in the tumor region following chemoradiation (Fig. 4).

4. Discussion

The goal of non-invasive radiological studies is to improve the management of malignant tumors by optimum characterization of a tumor and its response to therapy. Knowledge about immediate time- and dose-dependent associated changes in microscopic tumor tissue structures during combined hyperfractionated chemoradiation by using DWI can complement the information provided by traditional techniques. Spatial resolution of the ADC maps in this study calculated from echo-planar diffusion-weighted images with three different b-values was sufficient to identify the tumor region on ADC maps. The patient population in the present study was homogenous with regard to tumor entity (primary rectal carcinoma), tumor staging and grading (cT3, G2), and treatment regimen (standardized, preoperative, combined chemoradiation).

DWI is sensitive to microscopic translational motion of water molecules which occur in each voxel whereby signal attenuation is influenced not only by diffusion processes but also by perfusion and other kinds of motion, summarized as intravoxel incoherent motion (IVIM). If gross patient movement and various organ

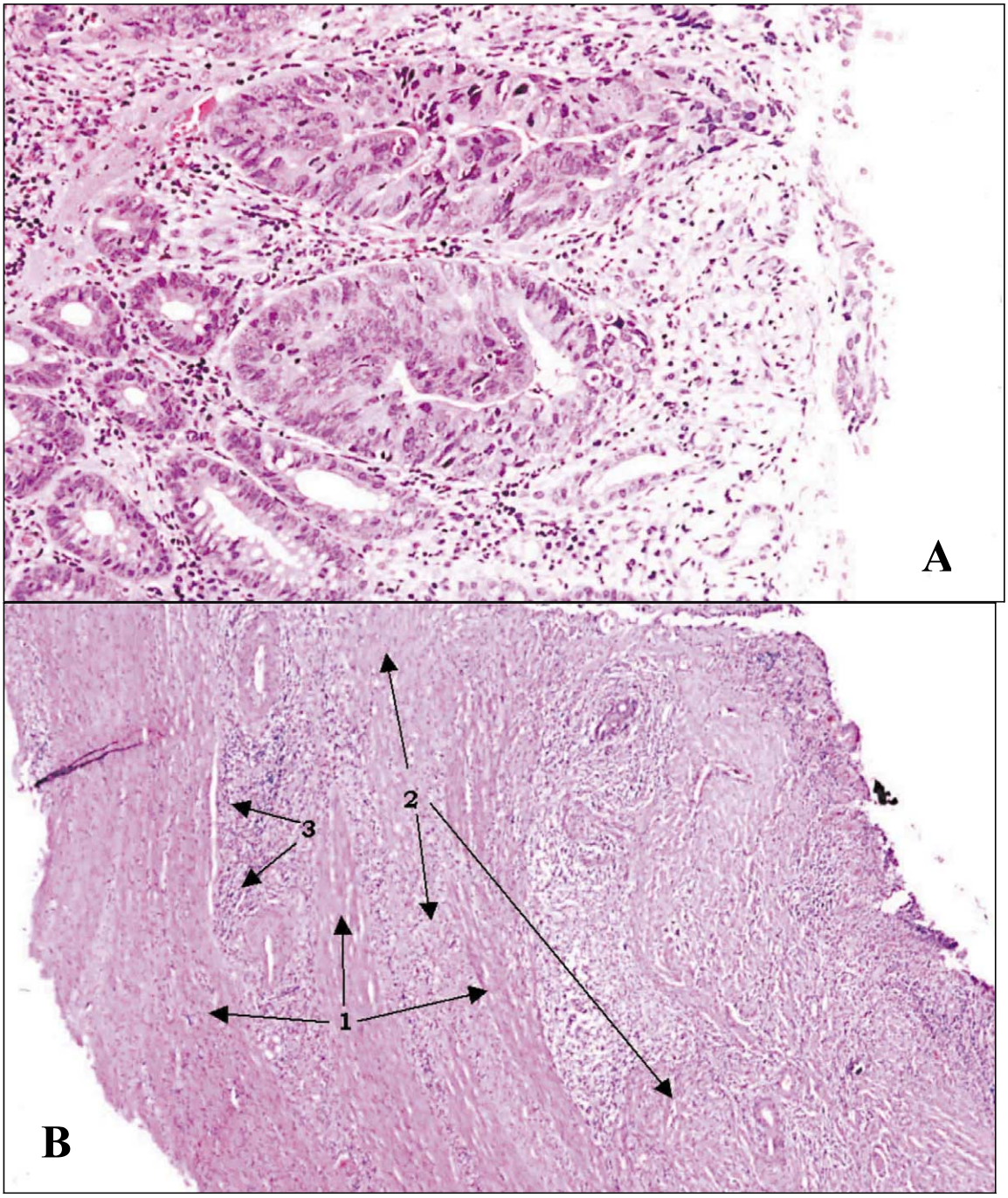

Fig. 4. Hematoxylin and eosin-stained slides, original magnification × 200. (A) Prior to chemoradiation: the tumor is characterized by glands with irregular lumina, lined by an atypical epithelium with hyper- and polychromatic nuclei showing stratification. The number of mitosis is increased. (B) Two weeks after chemoradiation: an ulcerated mucosa delineates the prior tumor area. The muscularis propria still contains muscle bundles (1) which are displaced by an increased amount of fibrous tissue (2). Note residual tumor nests and the dense lymphocytic infiltrate (3).

motions are excluded, high ADCs of a tumor region might be due to the influence of tumor perfusion [25,26]. Perfusion leads to water molecule motion during data acquisition and often shifts signal attenuation of DWI to higher values [27]. The results of perfusion imaging using the same patient population (diffusion-imaging started after four patients of the perfusion study; one patient added) at our institution were analyzed and published recently [1]. Dynamic T1 maps of the perfusion study revealed significantly increased PI (perfusion index) values in the first 2 weeks of treatment whereas changes in the 3rd and 4th weeks were not significant. There is no apparent connection with ADC changes in this present study and perfusion data obtained on the same patients. ADCs seem to represent mainly changes in water molecule mobility.

Table 2
Observed ADCs ($\times 10^{-3}$ mm^2/s) at weekly measurement points

Patient No.	Week 0	Week 1	Week 2	Week 3	Week 4
1	0.568	0.509	0.689	0.532	0.437
2	1.016	0.921	0.783	TME[a]	0.687
3	0.710	0.850	0.474	0.484	0.525
4	0.953	0.813	0.793	0.787	0.615
5	0.734	0.716	0.489	0.550	0.502
6	0.626	0.624	0.601	0.574	0.547
7	0.867	0.788	0.715	0.662	0.662
8	0.660	TME[a]	0.589	0.499	0.482
9	0.661	0.844	0.653	0.573	0.529

[a] Technical measurement error; data of patient No. 8 at 1st week and data of patient No. 2 at 3rd week missing due to technical error.

At the beginning of radiation therapy, a change of vessel permeability for water occurs [28], leading to interstitial edema and thus an increase of the ECV. However, the interstitial edema was observed only in two patients substantiated by elevated ADCs. How far diffusion data obtained in the early phase of therapy might be influenced by the presence of high interstitial fluid pressure [29] or oncotic pressure [30] within the tumor could not be answered at this time. Apoptosis can occur immediately following onset of therapy. Chinnaiyan et al. [15] monitored the effect of tumor-necrosis-factor-related apoptosis-inducing ligand and ionizing radiation in breast cancer cell lines with DWI and correlated the observed ADC increase with histologically proven apoptotic cell death. Their experimental study design used 15 Gy total radiation dose in three fractions, at 5 Gy per fraction. DWI measurements were obtained 1 week after treatment. In contrast, we employed conventional doses per fraction. Thus but less likely, another explanation for the observed two elevated ADC levels in our study might be ADC increase due to apoptotic cell death.

During the 2nd week, mean ADC decreased significantly. At that time 20 Gy was administered. Any ADC changes therefore can be explained by cell damage. The pathway of necrotic cell death shows cell swelling due to failure of the Na^+–K^+–ATPase pump. Cytotoxic edema arises from a shift of water from the ECV to the ICV [31]. Cell swelling as X-ray effect to intestinal cells has been described in various radiobiological studies [20,21,32]. The significant decrease of mean ADC starting at week 2 of therapy observed in our patient population appears to be consistent with cell injury.

Chemoradiation led to increased interstitial fibrosis as documented by postsurgical, pathohistological examination (Fig. 4). The limiting effect of fibers reduces free diffusion in the ECV. It can be hypothesized that at the end of therapy increasing development of fibrous connective tissue will decrease ADCs. Tissue anisotropy can be measured by DWI in muscle or white matter of the brain [15,16]. In normal anatomy, plane of orientation of the sensitizing gradient appears to be of importance. Measurements with sensitizing gradients parallel to the relative orientation of fiber bundles lead to higher ADCs. However, tumor tissue represents a mainly chaotic cellular structure and therefore intratumoral ADCs are not influenced by tissue anisotropy as recently shown by Lang et al. [13]. This study represents only measurements with diffusion weighting in slice selection.

Increased interstitial fluid pressure [29] and oncotic pressure [30] contribute to the suboptimal delivery of therapeutic agents in the tumor center. The ROIs of this study were similar between weeks 3 and 4. Since ADC levels continue to decrease during the same interval, it

Table 3
Results of Wilcoxon and Spearman tests

Results of Wilcoxon test by week	Results of Spearman r-test by week				
	0	1	2	3	4
0	–	0.643	0.467	0.500	0.750[a]
1	0.624	–	0.143	−0.036	0.524
2	0.028[a]	0.069	–	0.786[a]	0.617
3	0.012[a]	0.028[a]	0.123	–	0.810[a]
4	0.008[a]	0.012[a]	0.021[a]	0.063	–

[a] P value < 0.05.

can be cautiously postulated that this reflects the delayed response of the hypometabolic tumor center to combined chemoradiation.

Our observation of decreasing ADC levels with increasing radiation doses likely reflects the methodology used for this study. We defined the ROI as the volume likely containing viable tumor tissue throughout the course of treatment. Necrotic appearing areas were purposely excluded. Although some microscopically necrotic regions might have still been included in the ROI, their influence on ADC levels was likely small.

This study appears to have several limitations. (1) The sample size is limited to nine patients only. (2) The sample-slice with the largest tumor extension was selected for further analysis. The assumption has been made that the evaluation of a single slice is representative for the entire tumor. Other measurement techniques, e.g. tumor biopsies, are limited by a similar sampling problem. Additional studies are currently in progress in which we will compare a more extensive coverage of tumor through increase in sample rate to pre-existing values. (3) In our study design, we defined the intratumoral ROI as the region in which with highest certainty tumor tissue could be found at each measuring point. Manual drawing introduces some subjectivity. However, its advantage compared with a study using a stable geometric figure as ROI is the possibility of adjustment of the ROI to alterations in tumor diameter or cystic formation of tumor tissue during therapy.

In conclusion, this study demonstrated significant radiobiological changes in primary rectal carcinomas during therapy by the detection of changes in water mobility. Decreased ADC levels at completion of preoperative therapy were correlated with the development of intratumoral fibrosis. In addition to its routine neurological application, diffusion-weighted imaging has the potential as method to detect and quantify the early stage of this treatment effect.

Acknowledgements

The authors would like to thank the technicians of the Department of Radiotherapy and Radiooncology and the Department of Magnetic Resonance, University of Innsbruck, Austria, for their support during the course of this study. The presentation was supported in part by grants from Schering Germany and Schering Austria.

References

[1] DeVries A, Griebel J, Kremser C, Judmaier W, Gneiting T, Debbage P, Kremser T, Pfeiffer KP, Buchberger W, Lukas P. Monitoring of tumor microcirculation during fractionated radiation therapy in patients with rectal carcinoma: preliminary results and implications for therapy. Radiology 2000;217:385–91.

[2] Hawighorst H, Knapstein PG, Knopp MV, et al. Uterine cervical carcinoma: comparison of standard and pharmacokinetic analysis of time-intensity curves for assessment of tumor angiogenesis and patient survival. Cancer Res 1998;58:3598–602.

[3] Stejskal EO, Tanner JE. Spin diffusion measurements: spin echoes in the presence of time-dependent field gradients. J Chem Phys 1965;42:288–92.

[4] Le Bihan D, Turner R. Intravoxel incoherent motion using spin echoes. Magn Reson Med 1991;19:221–7.

[5] Tanner JE, Stejskal EO. Restricted self-diffusion of protons in colloidal systems by the pulsed gradient, spin-echo method. J Chem Phys 1968;49:1768–77.

[6] Le Bihan D. Molecular diffusion, tissue microdynamics and micro-structure. NMR Biomed 1995;8:375–86.

[7] Szafer A, Zhong J, Gore JC. Theoretical model for water diffusion in tissues. Magn Reson Med 1995;33:697–712.

[8] Duong TQ, Ackermann JJH, Ying HS, Neill J. Evaluation of extra- and intracellular apparent diffusion in normal and globally ischemic rat brain via ^{19}F NMR. Magn Reson Med 1998;40:1–13.

[9] Lansberg MG, Albers GW, Beaulieu C, Marks MP. Comparison of diffusion-weighted MRI and CT in acute stroke. Neurology 2000;54:1557–61.

[10] Pierpaoli C, Righini A, Linfante I, Tao-Cheng JH, Alger JR, Di Chiro G. Histopathologic correlates of abnormal water diffusion in cerebral ischemia: diffusion-weighted MR imaging and light and electron microscopic study. Radiology 1993;189:439–48.

[11] Chien D, Kwong KK, Gress DR, Buonanno FS, Buxton RB, Rosen BR. MR diffusion imaging of cerebral infarction in humans. Am J Neuroradiol 1992;13:1097–102.

[12] Els T, Eis M, Hoehn-Berlage M, Hossmann KA. Diffusion-weighted MR imaging of experimental brain tumors in rats. Magma 1995;3:13–20.

[13] Lang P, Wendland MF, Saeed M, et al. Osteogenic sarcoma: noninvasive in vivo assessment of tumor necrosis with diffusion-weighted MR-Imaging. Radiology 1998;206:227–35.

[14] Lyng H, Haraldseth O, Rifstad EK. Measurement of cell density and necrotic fraction in human xenografts by diffusion-weighted magnetic resonance imaging. Magn Reson Med 2000;43:828–36.

[15] Chinnaiyan AM, Prasad U, Shankar S, Hamstra DA, Shanaiah M, Chenevert TL, Ross BD, Rehemtulla A. Combined effect of tumor necrosis factor-related apoptosis-inducing ligand and ionizing radiation in breast cancer therapy. Proc Natl Acad Sci USA 2000;97:1754–9.

[16] Cleveland GG, Chang DC, Hazlewood CF, Rorschach HE. Nuclear magnetic resonance measurement of skeletal muscle. Biophys J 1976;16:1043–53.

[17] Chenevert TL, Brunberg JA, Pipe JG. Anisotropic diffusion in human white matter: demonstration with MR techniques in vivo. Radiology 1990;177:401–5.

[18] Chenevert TL, McKeever PE, Ross BD. Monitoring early response of experimental brain tumors to therapy using diffusion magnetic resonance. Clin Cancer Res 1997;3:1457–66.

[19] Zhao M, Pipe JG, Bonnett J, Evelhoch JL. Early detection of treatment response by diffusion-weighted ^{1}H NMR spectroscopy in a murine tumor in vivo. Br J Cancer 1996;73:61–4.

[20] Graham MM, Peterson LM. Functional measures of endothelial integrity and pharmacologic modification of radiation injury. In: Rubin DB, editor. The radiation biology of the vascular endothelium. Boca Raton, FL: CRC Press, 1997:40–63.

[21] Braun H. Cytologic changes in the intestine after radiation protection. In: Sullivan MF, editor. Gastrointestinal radiation injury. Monographs on nuclear medicine and biology, vol. 1. Copyright: Excerpta Medica Foundation, 1968:94–100.

[22] Murphy GP, O'Sullivan B, Sobin LH, Yarbo JW. Colon and rectum. In: Fleming ID, Cooper JS, Henson DE, Hutter RVP,

Kennedy BJ, Murphy GP, O'Sullivan B, editors. AJCC Cancer staging handbook, 5th ed. Philadelphia, PA: Lippincott-Raven, 1998:81–8.

[23] Gunderson LL, Russell AH, Llewellyn HJ, et al. Radiation and surgical techniques and value of small bowel films. Int J Radiat Oncol Biol Phys 1985;11:1379–93.

[24] Late effects consensus conference: RTOG/EORTC. Radiother Oncol 1995;35:5–7.

[25] Turner RT, Le Bihan D, Maier J, Vavrek R, Hedges LK, Pekar J. Echo-planar imaging of intravoxel incoherent motion. Radiology 1990;177:407–14.

[26] Yamada I, Aung W, Himeno Y, Nakagawa T, Shibuya H. Diffusion coefficients in abdominal organs and hepatic lesions: evaluation with intravoxel incoherent motion echo-planar imaging. Radiology 1999;210:617–23.

[27] Le Bihan D, Breton E, Lallemand D, Aubin ML, Vignaud J, Lavel-Jeantet M. Separation of diffusion and perfusion in intravoxel incoherent motion MR imaging. Radiology 1988;168:497–505.

[28] Withers HR, McBride WH. Biologic basis of radiation therapy. In: Berez CA, Brady LW, editors. Principles and practice of radiation oncology, 3rd ed. Philadelphia, PA: Lippincott-Raven, 1998:79–118.

[29] Boucher Y, Baxter LT, Jain RK. Interstitial pressure gradients in tissue-isolated and subcutaneous tumors: implications for therapy. Cancer Res 1990;50:4478–84.

[30] Stohrer M, Boucher Y, Stangassinger M, Jain RK. Oncotic pressure in solid tumors is elevated. Cancer Res 2000;60:4251–5.

[31] Sevick RJ, Kanda F, Mintorovitch J, Arieff AI, Kucharczyk J, Tsuruda JS, Norman D, Moseley ME. Cytotoxic brain edema: assessment with diffusion-weighted MR imaging. Radiology 1992;185:687–90.

[32] Rubin DB, Griem ML. The histopathology of irradiated endothelium. In: Rubin DB, editor. The radiation biology of the vascular endothelium. Boca Raton, FL: CRC Press, 1997:13–37.